

## Dynamics of step flow in a model of heteroepitaxy

A. A. Wheeler

*School Of Mathematics, University Walk, Bristol, BS8 1TW, United Kingdom*

C. Ratsch

*School of Physics, Georgia Institute of Technology, Atlanta, Georgia 30332*

A. Morales

*Department of Chemistry, California Institute of Technology, Pasadena, California 91126*

H. M. Cox

*Bellcore, 331 Newman Springs Road, Red Bank, New Jersey 07701*

A. Zangwill

*School of Physics, Georgia Institute of Technology, Atlanta, Georgia 30332*

(Received 3 March 1992)

We have investigated step-flow dynamics during growth of a periodic heterostructure on a vicinal surface, assuming different growth velocities for homoepitaxy and heteroepitaxy. Depending on the ratio of the two velocities for each of the two materials of the heterostructure, steps evolve from their initial distribution to closely spaced bunches of steps separated by wide terraces or they evolve to a common average terrace width. We present a mathematical analysis of the process in the latter regime and identify its boundary in a parameter space comprised of the two dimensionless velocity ratios. We verify this boundary by comparison with computer simulations and previously published experimental results.

### I. INTRODUCTION

In a recent paper, Cox and co-workers<sup>1</sup> introduced a generalization of the step-flow model of layer growth<sup>2</sup> designed to describe the deposition of two distinct materials (hereafter denoted by  $A$  and  $B$ ) onto a vicinal surface (one misoriented slightly from a principal crystallographic orientation, e.g.,  $3^\circ$  off  $[100]$ ). Briefly, their model recognizes a difference in lateral growth velocity for a material on itself (homoepitaxy) and on a different material (heteroepitaxy) *at the atomic level*. That is, the first atomic layer of growth of  $B$  on  $A$ , for instance, is allowed a different growth velocity than that of successive atomic layers of  $B$ , which are considered homoepitaxy ( $B$  on  $B$ ).

For simplicity, and consistent with their experimental conditions, a kinetically limited growth regime was assumed where each step was constrained to advance at a constant lateral velocity, depending only on the chemical identity of the material being grown and that of the layer immediately below. Thus, four parameters,  $V_{AB}$ ,  $V_{AA}$ ,  $V_{BA}$ , and  $V_{BB}$  (describing the lateral growth velocities of  $A$  on  $B$ ,  $A$  on  $A$ ,  $B$  on  $A$ , and  $B$  on  $B$ , respectively) characterize the dynamics of the process. In addition it was assumed that a step could not overtake the one below it as a minimum step-step separation was legislated.

Computer simulations, using the rules outlined above

and experimentally derived growth parameters, were quite successful in duplicating the evolution of an instability observed in the growth of an  $\text{In}_{0.53}\text{Ga}_{0.47}\text{As}$  multiple-quantum-well structure onto a vicinal surface<sup>1</sup> by vapor levitation epitaxy.<sup>3</sup> A cross-sectional transmission micrograph of the structure and the simulation from that study are repeated here, for reference, in Figs. 1(a) and 1(b), respectively. The micrograph of Fig. 1(a) shows alternating layers of InP (indicated by light areas) and  $\text{In}_{0.53}\text{Ga}_{0.47}\text{As}$  (indicated by dark areas) which start with a uniform thickness and are periodic in the growth direction. The interfaces become rough and the periodicity is disrupted as growth continues. The  $\text{In}_{0.53}\text{Ga}_{0.47}\text{As}$  regions ultimately coalesce into an array of quasi-one-dimensional wirelike filaments<sup>4</sup> with their longest dimensions normal to the plane of the figure. The simulation, shown in Fig. 1(b) evolves in a remarkably similar manner as surface steps bunch during growth to form macrosteps. Details of the experiment and simulation were given earlier in Cox *et al.*<sup>1</sup>

The behavior is characteristic of one of two modes of layer growth revealed by computer simulations of the alternate deposition of materials  $A$  and  $B$  onto a vicinal starting surface consisting of steps and terraces with randomly distributed widths. Depending on the choice of growth parameters, steps either (a) bunch and interfaces become rough, as shown in the experiment and simulation of Fig. 1, or (b) the terrace widths approach

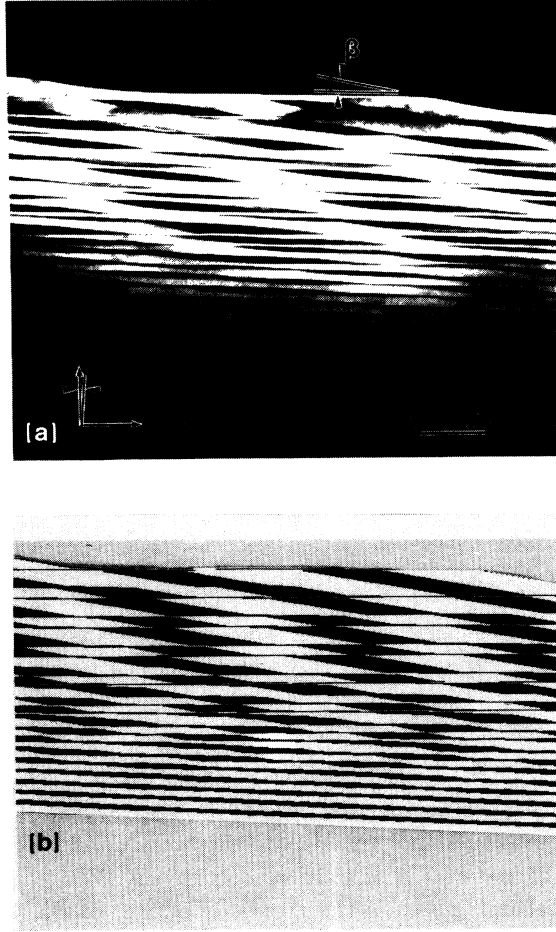


FIG. 1. (a) A cross-sectional transmission micrograph of InGaAs/InP multiple-quantum-well structure on a vicinal surface showing the effect of step bunching. (b) Numerical simulation using different lateral step velocities for heteroepitaxy and homoepitaxy.

a common value and interfaces become more planar as the growth proceeds. The two regimes are hereafter called the *step-bunching* and *terrace-width homogenization* regimes, respectively.

In this paper we present a mathematical analysis of the dynamics of step flow in the latter regime and identify the region in parameter space within which it occurs. In doing so we also establish the boundary of the step-bunching regime which is not currently amenable to an analytical treatment. We verify this boundary by comparison with computer simulations.

The terrace-width homogenization regime, while perhaps less interesting than that of step bunching for quantum wire growth, is technologically important because it leads to parallel planar interfaces which are crucial to modern semiconductor device technology. We note that terrace-width ordering has been examined in detail for the case of homoepitaxy in surface diffusion limited growth regimes.<sup>5-8</sup> That is a separate phenomenon, however, which can, depending upon the experimental conditions, either enhance or deter the ordering process specifically due to heteroepitaxy that we now address.

## II. THE MATHEMATICAL MODEL

We consider a model of heteroepitaxy in which two materials, denoted by  $A$  and  $B$ , grow alternately in layers. We assume that the surface is stepped and that growth only proceeds laterally from the edges of the monolayer-high steps. For simplicity, we model the situation when the steps all face in the same direction along which we orient the  $x$  axis.

Before proceeding we first introduce some notation. In Fig. 2 we show schematically a layer of  $B$  grown on  $A$ . Consider first the surface of  $A$ . The position of the steps along the  $x$  axis are given by the sequence  $\{x_j^n\}$  where the subscript  $j$  denotes the  $j$ th step and the superscript  $n$  denotes the  $n$ th layer. It is assumed that the

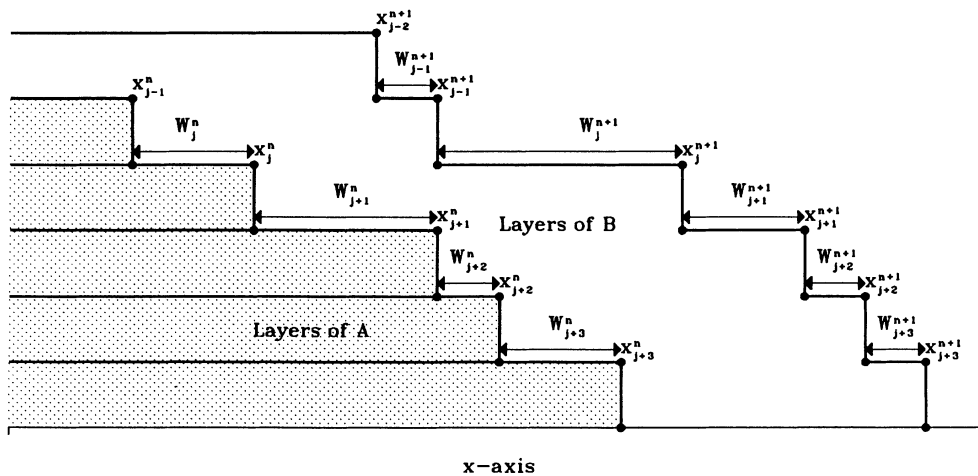


FIG. 2. Schematic diagram showing the notation for step positions and terrace widths of a vicinal surface of material  $A$  and the surface after step-flow growth of a layer of material  $B$ .

sequence of step positions  $\{x_j^n\}$  is monotonic increasing, i.e.,  $\dots x_{j-1}^n < x_j^n < x_{j+1}^n \dots$ . The width of the terrace between the steps at positions  $x_j^n$  and  $x_{j-1}^n$  is denoted by  $W_j^n$  and is therefore given by

$$W_j^n = x_j^n - x_{j-1}^n.$$

In order to develop our model we make the following assumptions.

(i) The growth of each material proceeds laterally, only from the step edges in the positive  $x$  direction, and the height of each monolayer of new material is equal to the step height.

(ii) The lateral velocity of growth of each monolayer depends on its composition ( $A$  or  $B$ ) and that of the underlying terrace ( $A$  or  $B$ ) upon which it grows.

(iii) The lateral growth velocity of a monolayer of material  $B$  on  $A$  is  $V_{BA}$ , and the velocity of growth of a monolayer of material  $A$  on  $B$  is  $V_{AB}$ . Similarly  $V_{AA}$  and  $V_{BB}$  are the lateral growth velocities of material  $A$  and material  $B$  on themselves, respectively.

(iv) The time during which growth occurs,  $T$ , is sufficiently long that every new step includes some homogeneous growth, i.e., material  $A$  on material  $A$  or material  $B$  on material  $B$ . For the case considered above of growth of a layer of  $B$  on a layer of  $A$  this requires  $TV_{BA} > \max(W_j^n)$ .

(v) Steps do not overtake other steps. This condition is violated when the steps bunch and we do not treat that situation here.

With these assumptions we now develop our mathematical model. Refer again to Fig. 2 and consider the growth of the  $j$ th step from position  $x_j^n$ . The growth of a step consists of two periods. The first called heterogeneous growth occurs when  $B$  grows on  $A$  and we denote this time period by  $T_{het}$ . The second period consists of homogeneous growth of  $A$  on  $A$  and we denote it by  $T_{hom}$ . The time for heterogeneous growth of the  $j$ th step is given by

$$T_{het} = \frac{W_{j+1}^n}{V_{BA}},$$

in which case the time for homogeneous growth is

$$T_{hom} = T - \frac{W_{j+1}^n}{V_{BA}}.$$

The position of the  $j$ th step at the end of the growth period  $x_j^{n+1}$  is therefore given by

$$x_j^{n+1} = x_j^n + T_{het}V_{BA} + T_{hom}V_{AA}$$

and so

$$x_j^{n+1} = x_j^n + W_{j+1}^n + \left(T - \frac{W_{j+1}^n}{V_{BA}}\right)V_{BB}. \quad (1)$$

Thus the new terrace width, which is given by  $W_{j+1}^{n+1} =$

$x_{j+1}^{n+1} - x_j^{n+1}$ , may be written using Eq. (1) as

$$W_{j+1}^{n+1} = \alpha_0 W_{j+1}^n + (1 - \alpha_0)W_{j+2}^n, \quad (2)$$

where  $\alpha_0 = V_{BB}/V_{BA}$ . We may conduct an identical analysis for the growth of the next layer in which a layer of  $A$  is grown on  $B$ . This gives

$$W_{j+1}^{n+2} = \alpha_1 W_{j+1}^{n+1} + (1 - \alpha_1)W_{j+2}^{n+1}, \quad (3)$$

where  $\alpha_1 = V_{AA}/V_{AB}$ . We now combine Eqs. (2) and (3) to obtain

$$W_j^{n+2} = A_0 W_j^n + A_1 W_{j+1}^n + A_2 W_{j+2}^n, \quad (4)$$

where

$$A_0 = \alpha_0 \alpha_1,$$

$$A_1 = [\alpha_0(1 - \alpha_1) + \alpha_1(1 - \alpha_0)],$$

$$A_2 = (1 - \alpha_0)(1 - \alpha_1),$$

which relates the terrace widths of the layer of material  $A$  at the  $n$ th time interval,  $W_j^n$ , to the terrace width of the layer of material  $A$  at its next occurrence,  $W_j^{n+2}$  (after an intervening step of the growth of a layer of  $B$ ). It is convenient to consider only the evolution of the terrace widths of  $A$  layers and thus we redefine the superscript  $n$  to represent the sequence of terrace widths between  $A$  layers, in which case Eq. (4) may be written as

$$W_j^{n+1} = A_0 W_j^n + A_1 W_{j+1}^n + A_2 W_{j+2}^n. \quad (5)$$

We call this the *step-flow equation*.

The step-flow equation has the solution  $W_j^n = C$  where  $C$  is a constant, which corresponds to growth where the steps are of uniform width and do not change between successive layers. Because the step-flow equation is linear it follows that if  $\widehat{W}_j^n$  and  $\widetilde{W}_j^n$  are solutions, then so is any linear combination of them;  $W_j^n = \mu \widehat{W}_j^n + \nu \widetilde{W}_j^n$ , where  $\mu$  and  $\nu$  are arbitrary real constants. By inspection of the step-flow equation it also admits solutions of the form

$$W_j^n = \mu(cn - i),$$

where  $c = \alpha_0 + \alpha_1 - 2$ . These represent traveling-wave solutions traveling with "speed"  $c$ . For a given layer ( $n$  fixed) the terrace widths depend linearly on the step index  $i$ . Clearly  $W_j^n$  changes sign for some  $i$  and thus the terrace widths pass through zero. This solution is therefore not physically meaningful.

We now consider spatially periodic solutions, which consist of a period of  $J$  terraces so that  $W_j^n = W_{j+J}^n$  for all  $j$ . We note that the sum  $A_0 + A_1 + A_2 = 1$ , in which case it can be shown that the total length of the period defined by  $L^n = \sum_{j=1}^{i=J} W_j^n$  is independent of  $n$ , and thus does not vary between successive layers of the same material. Hence the average terrace width  $l^n = L^n/J$  is constant throughout the evolution of the layers.

In general we are interested in whether the steps evolve from their initial distribution into either the step-bunching or step-homogenization regime, and how this depends on the two dimensionless parameters  $\alpha_0$  and  $\alpha_1$  and hence the four growth velocities  $V_{AB}, V_{AA}, V_{BA}$ , and  $V_{BB}$ . To investigate this we now conduct a Fourier analysis of the step-flow equation.

**A. Fourier analysis**

As above we consider periodic solutions consisting of  $J$  steps. We thus write the solution as a Fourier series

$$W_j^n = l + \sum_{k=1}^{k=J-1} a_k \lambda_k^n \exp(ji\beta_k) + \text{c.c.},$$

where

$$\beta_k = \frac{2\pi k}{J},$$

$i$  denotes the positive square root of  $-1$ ,  $\lambda_k$  represents the growth rate of the  $k$ th mode, and c.c. indicates the complex conjugate of the previous term. The constant  $l$  is the average terrace width of this periodic ensemble of steps, which we showed above is constant. Substituting this form into the step-flow equation gives the following expression for  $\lambda_k$ :

$$\lambda_k = A_0 + A_1 \exp(i\beta_k) + A_2 \exp(2i\beta_k), \tag{6}$$

which upon using the definition of the constants  $A_0, A_1$ , and  $A_2$  gives

---


$$|\lambda_k| = |\alpha_0 + (1 - \alpha_0)\exp(i\beta_k)| |\alpha_1 + (1 - \alpha_1)\exp(i\beta_k)| \text{ for } k = 1, \dots, J - 1. \tag{7}$$

The system will be stable and the step widths of all components of the solution decay as  $n$  increases if  $|\lambda_k| \leq 1$  for all  $k = 1, \dots, J - 1$ . In this case  $W_j^n \rightarrow l$ , as  $n \rightarrow \infty$ . We term this *homogenization* and the interface approaches a final state in which it is a uniform staircase where all the terrace widths are constant and equal to the average terrace width of the initial distribution. If, however, there exists a value of  $k$  such that  $|\lambda_k| > 1$ , the step widths will grow and ultimately the model may break down and we may expect step bunching to occur. Here we consider the conditions under which homogenization

occurs.

It is easy to show from Eq. (7) that if both  $\alpha_0 \leq 1$  and  $\alpha_1 \leq 1$  then  $|\lambda_k| \leq 1$  for all  $k$  and hence homogenization is assured, alternatively if both  $\alpha_0 > 1$  and  $\alpha_1 > 1$  then  $|\lambda_k| \geq 1$  for all  $k$  and homogenization does *not* occur. The remaining case is when one of  $\alpha_0$  and  $\alpha_1$  is less than or equal to unity and the other greater than unity. The step-flow equation is symmetric in  $\alpha_0$  and  $\alpha_1$  and so without loss of generality we may assume  $\alpha_0 \leq 1$  and  $\alpha_1 > 1$ . From Eq. (7) the requirement for homogenization that  $|\lambda_k| \leq 1$  for all  $k = 1, \dots, J - 1$  gives

---


$$[2\alpha_0(\alpha_0 - 1)(1 - \cos\beta_k) + 1] [2\alpha_1(\alpha_1 - 1)(1 - \cos\beta_k) + 1] \leq 1 \text{ for } k = 1, \dots, J - 1, \tag{8}$$

which can be shown to be satisfied providing

$$\frac{1}{2} - \frac{l_k}{2} \leq \alpha_0 \leq \frac{1}{2} + \frac{l_k}{2} \text{ for } k = 1, \dots, J - 1,$$

where

$$l_k = 2\sqrt{\frac{1}{4} - \frac{\alpha_1(\alpha_1 - 1)}{2\alpha_1(\alpha_1 - 1)[1 - \cos(\beta_k)] + 1}}, k = 1, \dots, J - 1$$

is the interval width. Thus for homogenization we require

$$\frac{1}{2} - \min_k \frac{l_k}{2} \leq \alpha_0 \leq \frac{1}{2} + \min_k \frac{l_k}{2}. \quad (9)$$

We observe that the interval width  $l_k$  is a monotonic decreasing function of  $\cos(\beta_k)$  and so its minimum is attained when  $\cos(\beta_k)$  is maximum, i.e.,  $k = 1$  or  $J - 1$ . Thus Eq. (9) requires  $\frac{1}{2} - \frac{l_1}{2} \leq \alpha_0 \leq \frac{1}{2} + \frac{l_1}{2}$ , i.e.,

$$\frac{1}{2} - \sqrt{\frac{1}{4} - \frac{\alpha_1(\alpha_1 - 1)}{2\alpha_1(\alpha_1 - 1)[1 - \cos(\frac{2\pi}{J})] + 1}} \leq \alpha_0 \leq \frac{1}{2} + \sqrt{\frac{1}{4} - \frac{\alpha_1(\alpha_1 - 1)}{2\alpha_1(\alpha_1 - 1)[1 - \cos(\frac{2\pi}{J})] + 1}}, \quad (10)$$

which is the condition for homogenization. We note that the interval length  $l_1$  is zero when  $\alpha_1 = \alpha_{crit}$  where

$$\alpha_1^{crit} = \frac{1}{2} + \sqrt{\frac{1}{4} + \frac{1}{2[1 + \cos(\frac{2\pi}{J})]}}. \quad (11)$$

For  $\alpha_1 > \alpha_1^{crit}$  there is no range of  $\alpha_0$  such that homogenization occurs. It is clear from Eq. (11) that  $\alpha_1^{crit}$  decreases as the total number of steps  $J$  increases. In fact in the limit  $J \rightarrow \infty$  Eq. (10) shows that the region of homogenization in  $(\alpha_0, \alpha_1)$  space is given by the interior of the circle of radius  $1/\sqrt{2}$  centered on  $(\frac{1}{2}, \frac{1}{2})$ . This implies that  $\alpha_1^{crit} \rightarrow 1/2 + 1/\sqrt{2} \approx 1.207$ , and so ho-

mogenization is not possible if  $\alpha_1^{crit} \geq 1/2 + 1/\sqrt{2}$ . In Fig. 3 we plot the region in  $(\alpha_0, \alpha_1)$  space in which homogenization occurs, for different values of  $J$ . Because the step-flow equation is invariant under the transformation  $\alpha_0 \rightarrow \alpha_1, \alpha_1 \rightarrow \alpha_0$ , the stability boundaries in the  $(\alpha_0, \alpha_1)$  plane have reflective symmetry about  $\alpha_1 = \alpha_0$ . Hence in Fig. 3 we only show them above this line of symmetry. The data below this line are discussed below in Sec. II B. The dashed curves show the stability boundaries for  $\beta_1 = \pi/3, \pi/2, 2\pi/3$ , i.e.,  $J = 6, 4$ , and  $3$ . It is clear that the region of homogenization decreases as the number of steps in the ensemble,  $J$ , increases. The solid curve gives the limiting case for the boundary of the homogenization region as  $J \rightarrow \infty$ . The convergence to the limit circle is evidently very rapid, and thus it provides the appropriate boundary for the physically relevant case of growth on a vicinal surface, where  $J$  is large.

## B. Computer simulation

The stability boundary was tested by comparison with results obtained by numerical simulation using the program developed earlier.<sup>1</sup> For example, the simulation shown in Fig. 1(b) was obtained using step velocities  $V_{AB} = 1.0, V_{AA} = 0.5, V_{BA} = 0.5$ , and  $V_{BB} = 1.0$ .

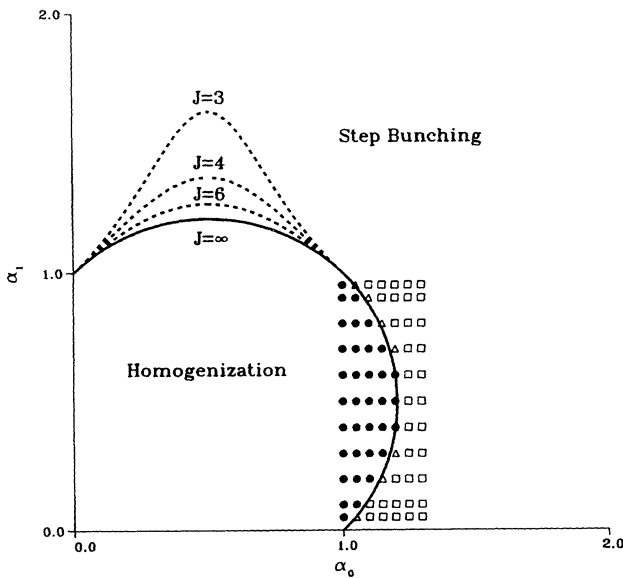


FIG. 3. The regions in  $(\alpha_0, \alpha_1)$  space in which homogenization will occur for different values of the  $J$ , the number of steps in a periodic ensemble. The solid curve represents the limiting case of a large number of steps,  $J \rightarrow \infty$ . The boundaries of the regions are symmetric about the line  $\alpha_1 = \alpha_0$ ; for the cases  $J = 3, 4$ , and  $6$  the boundary is only shown above this symmetry line. The data points below this line represent the results of the numerical simulations. A  $\bullet$  indicates the numerical simulation evolved to the homogenization regime, a  $\square$  that it evolved to the step-bunching regime, and a  $\triangle$  indicates that no determination of the regime could be made.

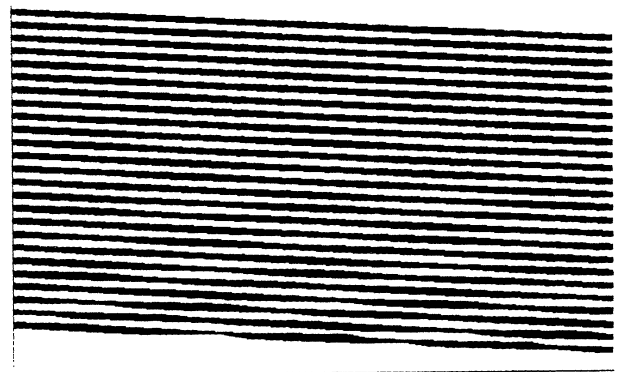


FIG. 4. Numerical simulation of a periodic structure grown on a very nonplanar vicinal surface using lateral step velocities for heteroepitaxy and homoepitaxy corresponding to the center of the terrace-width homogenization regime. The terrace widths quickly evolve to the initial average value, resulting in planar interfaces.

The corresponding values of  $\alpha_0 (= V_{BB}/V_{BA})$  and  $\alpha_1 (= V_{AA}/V_{AB})$  of 2.0 and 0.5, respectively, provide a point in  $(\alpha_0, \alpha_1)$  space, shown in Fig. 3, that is clearly in the step-bunching regime, consistent with the simulation and the experiment. In Fig. 4, we show the growth simulation of a periodic structure using relative step velocities of  $V_{AB} = 1.0, V_{AA} = 0.5, V_{BA} = 1.0,$  and  $V_{BB} = 0.5$ . In this case,  $\alpha_0$  and  $\alpha_1$  both equal 0.5 which is in the center of the regime of terrace-width homogenization. The positions of the steps, defining the initial surface, were placed at irregular intervals, simulating a very nonplanar surface. The terrace widths quickly adjust to their common average value, however, resulting in uniform layers with parallel interfaces, as predicted by our analysis.

We next conducted a series of similar simulations using different relative step velocities in order to verify the position of the boundary separating the two regimes of step-width ordering behavior. The results are summarized in the lower right section of the  $(\alpha_0, \alpha_1)$ -space plot of Fig. 3. The solid line is the circular boundary between the two regimes for  $J = \infty$ , which is appropriate for the large number steps used in the computer simulations. Pairs of  $\alpha_0$  and  $\alpha_1$  that result in step bunching are indicated by a  $\square$  and those that lead to terrace-width homogenization by a  $\bullet$ . The closer the values are to the boundary the slower the appearance of a state recognizable as one of the two regimes: If a trend was not apparent after about 100 periods the simulation was terminated and the point denoted by a  $\triangle$ . Excellent agreement between theory and the simulated is clearly apparent.

### III. DISCUSSION

It was the observation of step bunching that led Cox and co-workers to propose the model of step-flow heteroepitaxy<sup>1</sup> that we have treated mathematically. Our mathematical model is only strictly valid for the step-width homogenization regime. But, since it predicts step bunching for conditions outside the terrace-width homogenization regime, it provides a mathematical foundation for step bunching as well, even though it cannot model the dynamics after its onset. It should also be noted that intentional substrate misalignment to a vicinal orientation is not required for surface steps. Accidental misorientation, surface undulations, or even growth rate nonuniformities may produce the requisite steps. In addition, a periodic heterostructure with many interfaces was used in our analysis but some terrace-width readjustment obviously occurs at each interface.

In the earlier study,<sup>1</sup> a surface free-energy argument was used to predict that most superlattice structures should have one interface type for which the homoepitaxial step velocity exceeds the heteroepitaxial step velocity (using the general rule that if  $A$  wets  $B$ ,  $B$  will not wet  $A$ ,<sup>9</sup>) which, it was thought, would then lead to step bunching. It is clear from our present analysis, however, that there exists a region in  $(\alpha_0, \alpha_1)$  space where interface smoothing can result even if one of the homoepitaxial velocities exceeds the corresponding heteroepitaxial velocity.

We can consider, with caution, experimental evidence from other growth techniques for the heteroepitaxial step-flow model that we have analyzed. Molecular-beam epitaxy and organometallic vapor phase epitaxy usually operate in a mode where the step velocities are determined primarily from the arrival rate of adsorbed species from the terrace in front of the steps. This results in surface smoothing as growth proceeds even for homoepitaxy without heterointerfaces.<sup>5-8</sup> This effect would aid or mask any interface smoothing due to heteroepitaxy but tend to reverse step bunching caused by heteroepitaxy. These techniques can also operate with high group-V overpressure which limits the surface diffusion lengths, so that nucleation occurs between steps and step-flow behavior is lost. GaAs/AlGaAs superlattices are routinely observed with molecular-beam epitaxy to achieve more planar interfaces than a conventional single-material buffer provides.<sup>10,11</sup> A reasonable explanation for why a superlattice should be more effective at planarization than a standard buffer has been lacking. We conjecture that this interface smoothing occurs because of the relationship between the heteroepitaxy and homoepitaxy step-flow velocities in the step-flow homogenization regime, as described here.

A very careful and systematic study of GaInAs/InP and GaInAs/AlInAs superlattices grown by low-pressure organometallic vapor phase epitaxy was reported by Bhat and co-workers.<sup>12</sup> Excellent properties were obtained when InP layers were 5 nm or greater in thickness, but severe problems developed if the InP layers were reduced in thickness to 3 nm or less. They found these problems could be reduced by the use of low growth rates, growth interruptions after InP growth, a substrate oriented as close to exact (100) as possible, and minimization of growth rate nonuniformities. Through a process too extensive to be described here, they eliminated all conventional explanations and concluded that the results were all consistent with the model of step-flow heteroepitaxy as proposed by Cox *et al.*<sup>1</sup> Step bunching was occurring at the initial stage of growth of InP on InGaAs because the lateral growth velocity of InP on InP was greater than that of InP on InGaAs. If sufficiently thick layers were grown, the bunching was eliminated by the mechanism discussed earlier.<sup>5-8</sup>

These examples indicate that the general behavior predicted by the analysis given here may be applicable to growth techniques that are not kinetically limited and do not even come close to meeting our initial simplifying assumptions. Detailed agreement will obviously require a more complicated analysis that allows for growth limited by surface migration.

### IV. SUMMARY

We have presented a mathematical analysis of the step-flow dynamics of the growth of a periodic heterostructure on a vicinal surface using different growth velocities for homoepitaxy and heteroepitaxy, as proposed earlier by Cox *et al.*<sup>1</sup> Depending on the choice of those velocities, steps evolve from their initial distribution to either

closely spaced bunches of steps, separated by wide terraces, or they evolve to a common average terrace width. We have treated the process in the latter regime and identified the region in parameter space where it occurs.

The location of the boundary separating the two regimes was verified by numerical simulation. Excellent agreement between theory and the simulations was ob-

tained. The analytical results are strictly valid only for the terrace-width homogenization regime. Since the computer simulations could be used in either regime they provide a link between the theoretical results and experimentally observed interface roughening due to step bunching, previously reported.<sup>1</sup>

---

<sup>1</sup>H. M. Cox *et al.*, *Appl. Phys. Lett.* **57**, 611 (1990).

<sup>2</sup>W. K. Burton, N. Cabrera, and F. C. Frank, *Philos. Trans. R. Soc. London Ser. A* **243**, 299 (1951).

<sup>3</sup>H. M. Cox, S. G. Hummel, and V. G. Keramidas, *J. Cryst. Growth* **79**, 900 (1986).

<sup>4</sup>S. J. Allen, Jr. *et al.*, *J. Appl. Phys.* **66**, 1222 (1989).

<sup>5</sup>R. L. Schwoebel and E. J. Shipsey, *J. Appl. Phys.* **37**, 3682 (1966).

<sup>6</sup>Y. Tokura, H. Saito, and T. Fukui, *J. Cryst. Growth* **94**, 46 (1989).

<sup>7</sup>H. J. Grossman, F. W. Sinden, and L. C. Feldman, *J. Appl. Phys.* **67**, 74 (1990).

<sup>8</sup>A. K. Myers-Beaghton and M. R. Wilby, *J. Phys. A* **24**, L35 (1991).

<sup>9</sup>M. Copel, M. C. Reuter, E. Kaxiras, and R. M. Tromp, *Phys. Rev. Lett* **63**, 632 (1989).

<sup>10</sup>T. J. Drummond *et al.*, *Appl. Phys. Lett.* **42**, 615 (1983).

<sup>11</sup>K. Ploog, A. Fischer, L. Tapfer, and B. F. Feuerbacher, *J. Cryst. Growth* **111**, 344 (1991).

<sup>12</sup>R. Bhat *et al.*, *J. Cryst. Growth* **110**, 353 (1991).

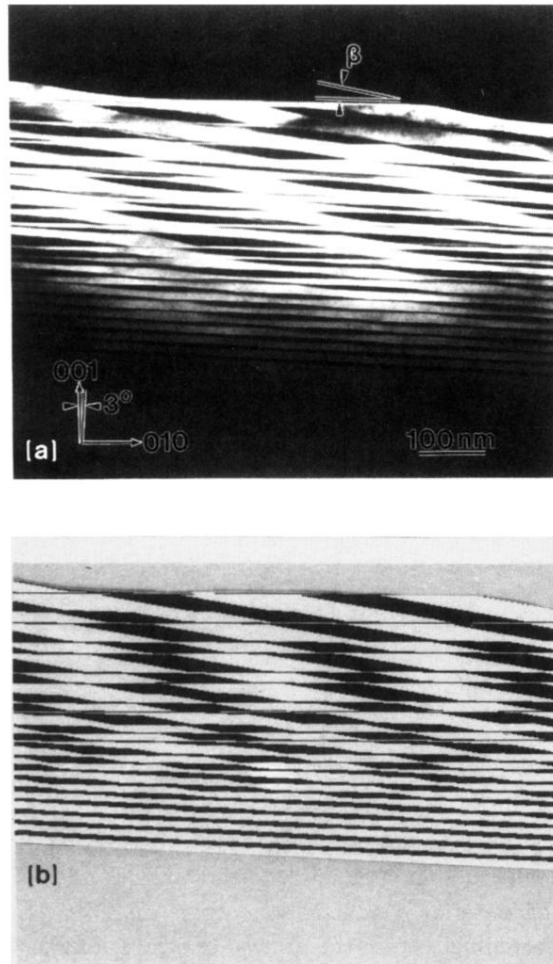


FIG. 1. (a) A cross-sectional transmission micrograph of InGaAs/InP multiple-quantum-well structure on a vicinal surface showing the effect of step bunching. (b) Numerical simulation using different lateral step velocities for heteroepitaxy and homoepitaxy.

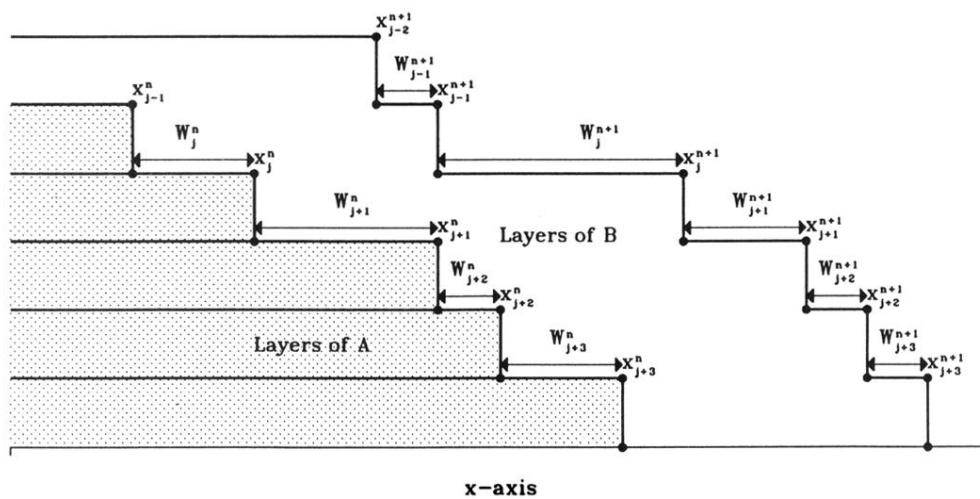


FIG. 2. Schematic diagram showing the notation for step positions and terrace widths of a vicinal surface of material *A* and the surface after step-flow growth of a layer of material *B*.